Evaluation of Northern Hemisphere surface wind speed and wind power density in multiple reanalysis datasets

Haozeyu Miao [a, c], Danhong Dong [c], Gang Huang [b, c, e, *], Kaiming Hu [c, d], Qun Tian [c, e], Yuanfa Gong [a]

[a] College of Atmospheric Sciences, Chengdu University of Information Technology, Chengdu, 610225, China
[b] Laboratory for Regional Oceanography and Numerical Modeling, Qingdao National Laboratory for Marine Science and Technology, Qingdao, 266237, China
[c] State Key Laboratory of Numerical Modeling for Atmospheric Sciences and Geophysical Fluid Dynamics, Institute of Atmospheric Physics, Chinese Academy of Sciences, Beijing, 100029, China
[d] Center for Monsoon System Research, Institute of Atmospheric Physics, Chinese Academy of Sciences, Beijing, 100029, China
[e] University of Chinese Academy of Sciences, Beijing, 100049, China

ARTICLE INFO

ABSTRACT

Reanalysis products have become more and more popular for wind energy scientific community to analyze the wind speed variability and get long-term wind power estimations. The present study evaluates the biases of near-surface wind speed and wind power density in four of the most reputable reanalysis datasets, which include ERA-Interim, JRA-55, CFS and MERRA-2. The results indicate that the abilities of reanalysis products to reproduce the variabilities of wind speeds are different in different regions. JRA-55 and CFS offer the best estimates of annual and seasonal variabilities of surface wind speeds over the Northern Hemisphere. In detail, JRA-55 is the best to reproduce surface wind speeds in Asia, CFS has the best performance in Europe, and MERRA-2 just can reproduce the central part of North America. All the four datasets show decreasing tendencies in surface winds over the Northern Hemisphere during 1980–2016, although the trends are largely diverse among them. The most significant disagreements of wind speed trends are encountered between JRA-55 and MERRA-2, which are likely related to the different methodologies from the lowest model level that reanalyses use. The main drivers of wind speed trends are the changes of large-scale circulation, urbanization, and aerosol emissions.

© 2020 Elsevier Ltd. All rights reserved.

1. Introduction

Since conventional energy such as coal and oil has brought serious environmental problems, the development of renewable energy has been widely concerned around the world and has become a hot spot in the international energy field [1]. Wind energy is an important renewable energy resource [2], which is rapidly developed around the world due to its safety, cleanliness and abundance [3]. According to the latest preliminary statistics of the World Wind Energy Association (WWEA), the cumulative installed capacity of global wind power reached 597 GW in 2018, which accounted for 6% of global electricity demand. In 2018 alone,

50.1 GW of wind power installed capacity was added worldwide, among which 21 GW were installed in China, and therefore China exceeded 200 GW of total wind power installation. The United States ranked second with 96 GW, followed by Germany (59 GW), India (35 GW), Spain (23 GW), the United Kingdom (20.7 GW) and France (15.3 GW) [4].

In order to achieve economical production of electricity, wind energy resource in different locations needs to be investigated in detail [5]. Wind power density is proportional to the cube of wind speed [6]. As a widely used indicator to describe the frequency distribution of wind speed, the Weibull probability density function is a crucial factor in wind resource assessment [7–12]. Young et al. [13] found a general growing trend of global oceanic wind speed over the past 23 years since the 1990s by using a database of calibrated and validated satellite altimeter measurements. On land, however, surface wind speeds have been decreasing in most parts of the Northern Hemisphere, including North America, Europe and

Asia, over the past four decades [14]. Recently, this phenomenon has also been confirmed by many studies. In most land areas around the world, surface wind speeds have generally declined [15−19]. Rehman [20] analyzed long-term wind speed trends of 28 meteorological stations in Saudi Arabia using the Mann-Kendall test and linear regression method, providing important indicators for the country's future wind regime. Surface wind speed changes not only play an important role in assessing wind energy, but also in atmospheric evaporation and air pollution dispersal [21−23]. Multiple researches have also assessed the global and regional wind energy based on the observations and reanalysis data [24−27], and prediction of future wind energy using forecast models [28−32]. Evaluation of wind speed and wind power density can provide a reference for the development of wind energy resources, which will reduce the energy and environmental crisis and promote the sustainable development of human society.

Due to the spatial and temporal sampling limitations of observational datasets, various reanalysis products have been greatly developed and widely used for climatological research and have become a tool for wind energy scientific community to require the long-term variability of surface wind speed [2,33−35] and also use as input for the wind power production modelling [36−38]. However, because of the systematic biases and uncertainties caused by the data assimilation and physical process in the forecast model, it is necessary to evaluate the quality of reanalysis datasets by comparing with observations. Various meteorological variables such as air temperature, wind speed, precipitation, snow depth, soil temperature and moisture have been widely evaluated based on different reanalysis datasets [39−44]. According to previous studies, reanalysis data is unlikely to perform well in all regions or all periods [45−48]. For example, it is found that the wind speed from reanalysis data is generally lower than the sounding data in climatological characteristics [49]. Kim et al. [50] evaluated the applicability of wind energy from CFSR, ERA-Interim, MERRA and MERRA-2 in southwestern South Korea, and found that the wind power density difference among these four reanalyses was more than 20%. This magnitude of difference cannot be neglected in the wind resource assessment. As such it is crucial to select an appropriate reanalysis dataset. Torralba et al. [2] found an increasing trend of global wind speed over the ocean and decreasing over land based on three reanalysis datasets, while lacking the comparison with observations. The authenticity of the reanalysis is yet to be verified.

The wind energy resource over the Northern Hemisphere is susceptible to climate change. The strong winds from intense wind storms could lead to safety problems, while the declining trend of wind speed would result in economic losses when it cannot meet the demand of electricity supply [2,51]. To our knowledge, there is still no published study that focuses on a comprehensive and systematic comparison of wind field data from the observations and reanalysis datasets over the whole Northern Hemisphere, where three major wind power markets including North America, Europe and Asia are located [52]. Therefore, evaluations of the reliability and accuracy of reanalysis datasets over the Northern Hemisphere and different regions need to be carried out, which are important for the development of wind energy resources, as well as the global and regional climate researches.

In this paper, our study mainly focuses on the analysis of the differences between the observations and reanalyses from the aspects of climatological characteristics, interannual variability and long-term linear trend, to evaluate the applicability of wind speeds and wind power density of reanalysis datasets over the Northern Hemisphere. The framework of this paper is as follows. The reanalysis and observational datasets and methods used are introduced in section 2. Sections 3 and 4 show the results of the comparative analysis of reanalyses and observations over the Northern Hemisphere and different regions, respectively. Discussion and conclusion follow in section 5 and section 6, respectively.

2. Data and method

2.1. Data

2.1.1. OBS

The observational data (OBS) used in this study is from two sources:

The first is the Integrated Surface Database (ISD) [53] from the National Centers for Environmental Information (NCEI), National Oceanic and Atmospheric Administration (NOAA) in 1998, containing global surface hourly observations of hundreds of meteorological parameters from more than 100 original data sources. ISD includes more than 20,000 stations worldwide, of which more than 11,000 active stations are updated daily in the database at present. ISD contains 54 quality control (QC) algorithms for processing each observational data through a series of validity checks, extreme value checks, internal (within observation) continuity checks, and external (versus another observation for the same station) consistency checks. Surface wind speeds at 10 m are selected for this study, and several QC processes are conducted to ensure the quality of the wind speed time series. Firstly, removing stations that were moved from one place to a distant other place, retaining the stations with less than 0.02° (about 2 km) in horizontal relocation. Then removing stations with large gaps, keeping records covering more than 360 days a year.

The other dataset is from Daily Climate Data from Chinese Surface Stations (V3.0), which is provided by the China Meteorological Data Service Center (CMDC), Chinese Meteorological Administration (CMA), including daily values from 824 Chinese surface stations. Through a series of QC processes including extreme value checks, internal consistency checks, external consistency checks and manual verification and correction, surface wind speeds at 10 m are chosen as well.

After QC processes, only 687 stations are retained from NCEI ISD and 351 stations from the CMDC daily surface observation V3.0 for the period of 1980−2016.

2.1.2. ERA-Interim

The ERA-Interim dataset [54] is the third-generation reanalysis dataset produced by the European Center for Medium-Range Weather Forecasts (ECMWF) for the period since 1979. This is based on the assimilation of conventional data and satellite observations and coupled with atmospheric, ocean and land models, providing global users with the latest global atmospheric numerical forecast reanalysis data. ERA-Interim, with the latest four-dimensional variation data assimilation (4D-Var), combines improved moisture analysis, satellite data error correction and other technologies to improve the quality of reanalysis data. Thus, it is regarded as an updated and improved version of ERA-15 and ERA-40. It contains 60 model levels and 37 pressure levels, from surface up to 0.1 hPa. Here the monthly means of daily 6-hourly 10 m wind speed are adopted with $0.75° \times 0.75°$ resolution.

2.1.3. JRA-55

The JRA-55 dataset [55] is the second Japanese global atmospheric reanalysis project provided by the Japan Meteorological Agency (JMA), which covers the period from 1958 when the global radiosonde observing system was established. It is an upgraded version of JRA-25, which fixes and alleviates many of the deficiencies in JRA-25 and extends back to 1958, while JRA-25 only covers from 1979 to 2004 [56]. The assimilation system of JRA-55

was upgraded, and the global spectrum mode is used as the numerical prediction model. Meantime, these improvements are achieved by higher spatial resolution of 60 km (TL319 L60), the top layer up to 0.1 hPa, a new radiation scheme, 4D-Var of satellite radiation and variation deviation correction (VarBC), as well as the introduction of time-varying concentration greenhouse gases. Daily 6-hourly wind speeds at 10 m with $1.25° \times 1.25°$ resolution are used in this study.

2.1.4. CFS

CFSR and CFSv2 are the newest global, high-resolution reanalysis datasets, released by NCEP. CFSR is the third reanalysis data using the global high-resolution atmospheric-ocean-land surface-sea ice coupling system [57] with a time coverage of 1979−2010. CFSv2 is the extended product of CFSR, starting at 2011, with higher resolution. In our study, u and v components of wind at 10 m of one-hourly forecasts with $0.5° \times 0.5°$ resolution are selected.

2.1.5. MERRA-2

MERRA-2 [58], produced by NASAs Global Modeling and Assimilation Office (GMAO), is the latest atmospheric reanalysis dataset of the modern satellite era providing data beginning at 1980. As a timely replacement of MERRA [59], the GEOS atmospheric model [60,61] and the GSI analysis scheme [62] are the pivotal components of the system. The spatial resolution of MERRA-2 is about 50 km in the latitudinal direction and 72 hybrid-eta levels from the surface to 0.01 hPa. MERRA-2 maintains some of the same basic features of MERRA, and it has important updates and improvements in terms of prediction models, analysis algorithms, observation systems, and radiation assimilation. In this study, one-hourly 10 m eastward wind and northward wind on a grid with 576 points in the longitudinal direction and 361 points in the latitudinal direction ($0.625° \times 0.5°$) are chosen.

In this study, the 10 m wind is used as a proxy to analyze the variability of wind because it has been shown that reanalyses can reproduce the characteristics of 10 m wind speed at spatial and temporal scales [2,63]. All of these four reanalysis datasets are compared with the observational dataset during the period from 1980 to 2016.

2.2. Method

2.2.1. Calculation of wind power density

The wind power density (WPD) is defined as the kinetic energy through which the airflow flows, so the wind power density passing through the unit area vertically in a unit of time can be expressed as:

$$WPD = \frac{1}{2}\rho V^3 \tag{1}$$

where *WPD* is the wind power density (unit: Wm^{-2}), *V* is the wind speed (unit: ms^{-1}), and ρ is the air density (unit: kgm^{-3}). The calculated monthly mean wind speeds of each data are used for the calculation.

2.2.2. Spatial interpolation method

Bilinear interpolation, which has been proven to offer a slight improvement compared with other approaches (such as nearest-neighbor, nine-point average), is adopted to interpolate the gridded data from reanalyses to each meteorological station location. As one of the most commonly used resampling techniques for two-dimensional distributed data, bilinear interpolation is widely used to interpolate variables which are smoothly varying, based on the linear interpolation in the direction of the variables of radius and

azimuth [64]. Let (ρ, θ) be the polar coordinates of the interest point that lying inside the curvilinear trapezoid with four neighboring vertices $Z_{i,j}, Z_{i+1,j}, Z_{i,j+1}$ and $Z_{i+1,j+1}$, *R* be the range of the radar, and N_φ and N_r be the dimensions of the reflectivity *Z*. The value of the point obtained by interpolation is determined by the values of four adjacent vertices:

$$Z = [1 - \varphi\varphi]\begin{bmatrix} Z_{i+1,j+1} & Z_{i+1,j} \\ Z_{i,j+1} & Z_{i,j} \end{bmatrix}\begin{bmatrix} 1 - r \\ r \end{bmatrix} \tag{2}$$

$$\varphi = \theta - \frac{2\pi(i-1)}{N_\varphi}, r = \rho - \frac{R(j-1)}{N_r} \tag{3}$$

φ is the relative azimuth and *r* is the relative radius.

2.2.3. Basic statistical and error analysis

Four reanalysis datasets are evaluated to the observational dataset for the period of 1980 through 2016. Monthly means from these datasets are used to evaluate the climatology and time series of wind speed and wind power density. In this study, several statistical indices are introduced to evaluate the annual and seasonal characteristics of wind speed and wind power density. Here is the conventional definition of the four seasons: spring (March−May; MAM), summer (June−August; JJA), autumn (September−November; SON), and winter (December−February; DJF).

Bias is used to calculate the difference between the reanalysis data and the observed data:

$$BIAS = \frac{1}{N}\sum_{i=1}^{N}(S_i - O_i) \tag{4}$$

Standard deviation (SD) represents the interannual variability of wind speed and wind power density:

$$SD = \sqrt{\frac{1}{N}\sum_{i=1}^{N}(X_i - \overline{X})^2} \tag{5}$$

The correlation coefficient (CC) is adopted to study the degree of linear correlation between the reanalysis and the observed wind speed/wind power density:

$$CC = \frac{\sum_{i=1}^{N}(S_i - \overline{S})(O_i - \overline{O})}{\sqrt{\sum_{i=1}^{N}(S_i - \overline{S})^2}\sqrt{\sum_{i=1}^{N}(O_i - \overline{O})^2}} \tag{6}$$

Root mean square difference (RMSD) is a measurement of the deviation between the reanalysis data and the observed data:

$$RMSD = \sqrt{\frac{1}{N}\sum_{i=1}^{N}(S_i - O_i)^2} \tag{7}$$

Here, X_i is the wind speed/wind power density series and $\overline{X}$ is the average value of each dataset. S_i is the wind speed/wind power density series of the reanalysis data, O_i is the observed wind speed/wind power density series, $\overline{S}$ and $\overline{O}$ are the average values of the reanalysis and observed data, respectively. And *N* is the corresponding sample size.

The least-square method is used to calculate the univariate linear trend (LT) of wind speed/wind power density. For the x_i of wind speed series, the corresponding time t_i and the error term u_i:

$$x_i = a + bt_i + u_i \tag{8}$$

$$\widehat{b} = \frac{\sum_{i=1}^{N} x_i t_i - \frac{1}{N} \left(\sum_{i=1}^{N} x_i \right) \left(\sum_{i=1}^{N} t_i \right)}{\sum_{i=1}^{N} t_i^2 - \frac{1}{N} \left(\sum_{i=1}^{N} t_i \right)^2}, \widehat{a} = \overline{x} - \widehat{b}\overline{t} \qquad (9)$$

b is the regression coefficient, a is a constant, and $\widehat{b}$ and $\widehat{a}$ are respectively the estimated values of b and a based on the least-square method. $\overline{x}$ and $\overline{t}$ are respectively the average values of wind speed and time.

2.2.4. Temporal and spatial averaging

The wind speed and wind power density are evaluated on the time scales of multiyear mean, annual mean and seasonal mean based on the monthly mean values. First, monthly mean values are computed from 1-hourly, 6-hourly or daily values in each dataset for each station. Then, for each site the multiyear mean, bias, root mean square difference, standard deviation, linear trend and correlation coefficient are calculated using monthly means. The values at different time scales can be obtained by further temporal averaging. Finally, spatial averaging is performed for all stations or those in different regions after temporal averaging.

3. Comparison of multiple datasets over the Northern Hemisphere

3.1. Annual wind speed and wind power density variations

The spatial distribution of all stations in the NCEI-CMDC dataset is shown in Fig. 1. There are 1038 stations in total, most of them are located in the Northern Hemisphere. And the Northern Hemisphere region has been divided into these three regions: Europe $(30 - 72°\mathrm{N}, 20°\mathrm{W} - 50°\mathrm{E}, 224 \text{ stations})$, Asia $(0 - 55°\mathrm{N}, 50° - 150°\mathrm{E}, 531 \text{ stations})$ and North America $(20 -$

$55°\mathrm{N}, 60 - 140°\mathrm{W}, 215 \text{ stations})$, since they are the three largest wind power markets mentioned above [52].

Fig. 2 shows the time series and linear trends of regional mean wind speeds and wind power density over all 1038 stations based on the four reanalysis datasets and observations. It shows that cyclical patterns and turning points are similar in most datasets, suggesting that interannual fluctuations are captured well by most datasets. Moreover, all datasets reflect declining trends between 1980 and 2016, despite the magnitudes of negative trends are inconsistent. The trends of wind speeds or wind power density in JRA-55 and CFS are similar to the observations, while the trends in MERRA-2 and ERA-Interim are much weaker than the observed data. In addition, the climatological values of wind speed and wind power density in MERRA-2, ERA-Interim and CFS are higher than the observations. JRA-55 is more consistent with the observational results in describing the wind power density, but exhibits significant negative anomalies for wind speed.

Furthermore, several statistic indices are selected to assess the overall quality of the four reanalysis datasets compared to the observations, shown in Table 1 for wind speed and Table 2 for wind power density. The multiyear means of wind speeds and wind power density from observations are 3.495 ms^{-1} and 44.039 Wm^{-2}, respectively. Both of these two variables have downward trends for the period of 1980−2016 over the Northern Hemisphere for all datasets. But the downtrend values from all reanalyses are smaller than the observations, which indicates that these four reanalysis datasets underestimate the observed decline in wind speed and wind power density. According to the results of significance test, the trends of wind speed from all datasets are statistically significant at the 1% level. In terms of wind power density, except for MERRA-2, trends from the other three datasets pass the 95% significance test. For the wind speed (Table 1), except JRA-55, the other three reanalyses show positive biases from the observed results. In general, JRA-55 is the most relevant to the observed results and CFS
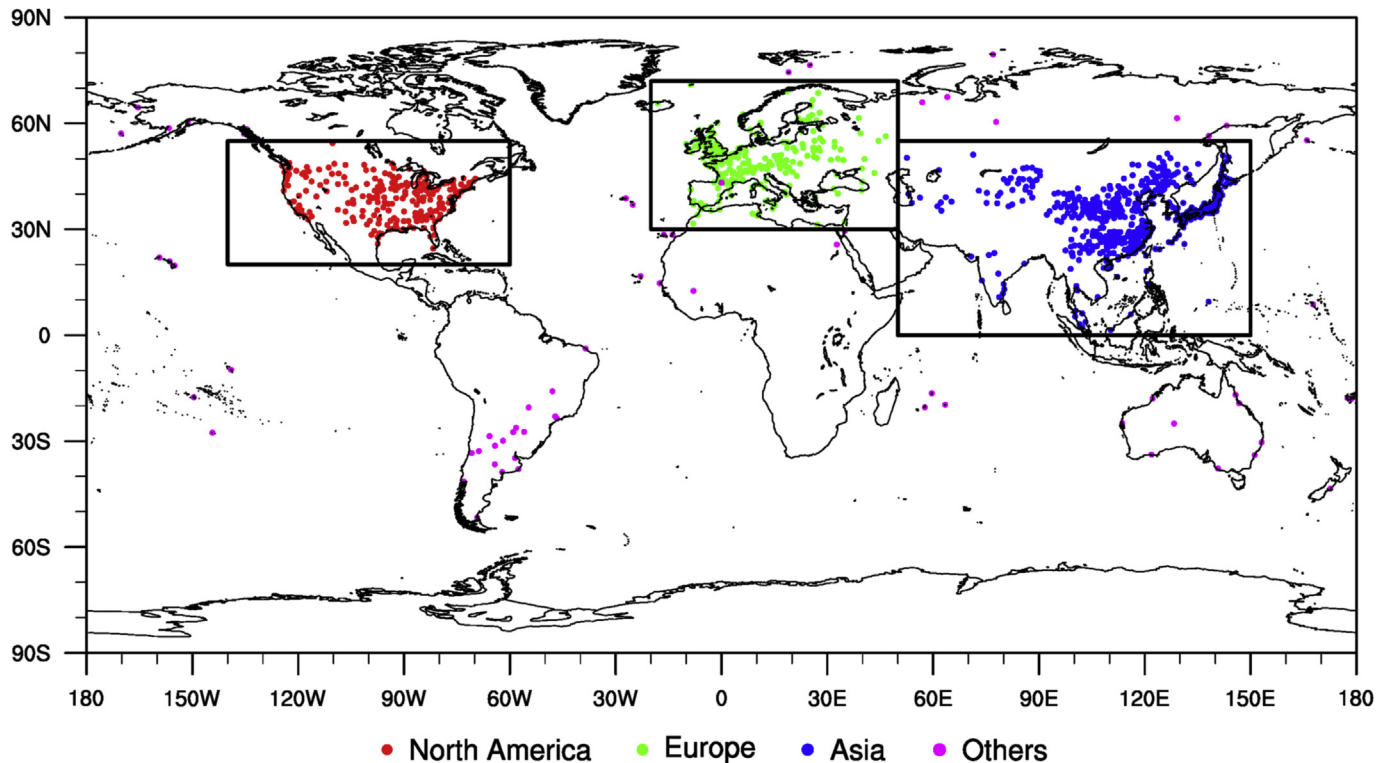

Fig. 1. Spatial distribution of stations using in this study. There are three major regions: North America (*reddots*), Europe (*greendots*), Asia (*bluedots*), and other stations (*pinkdots*).
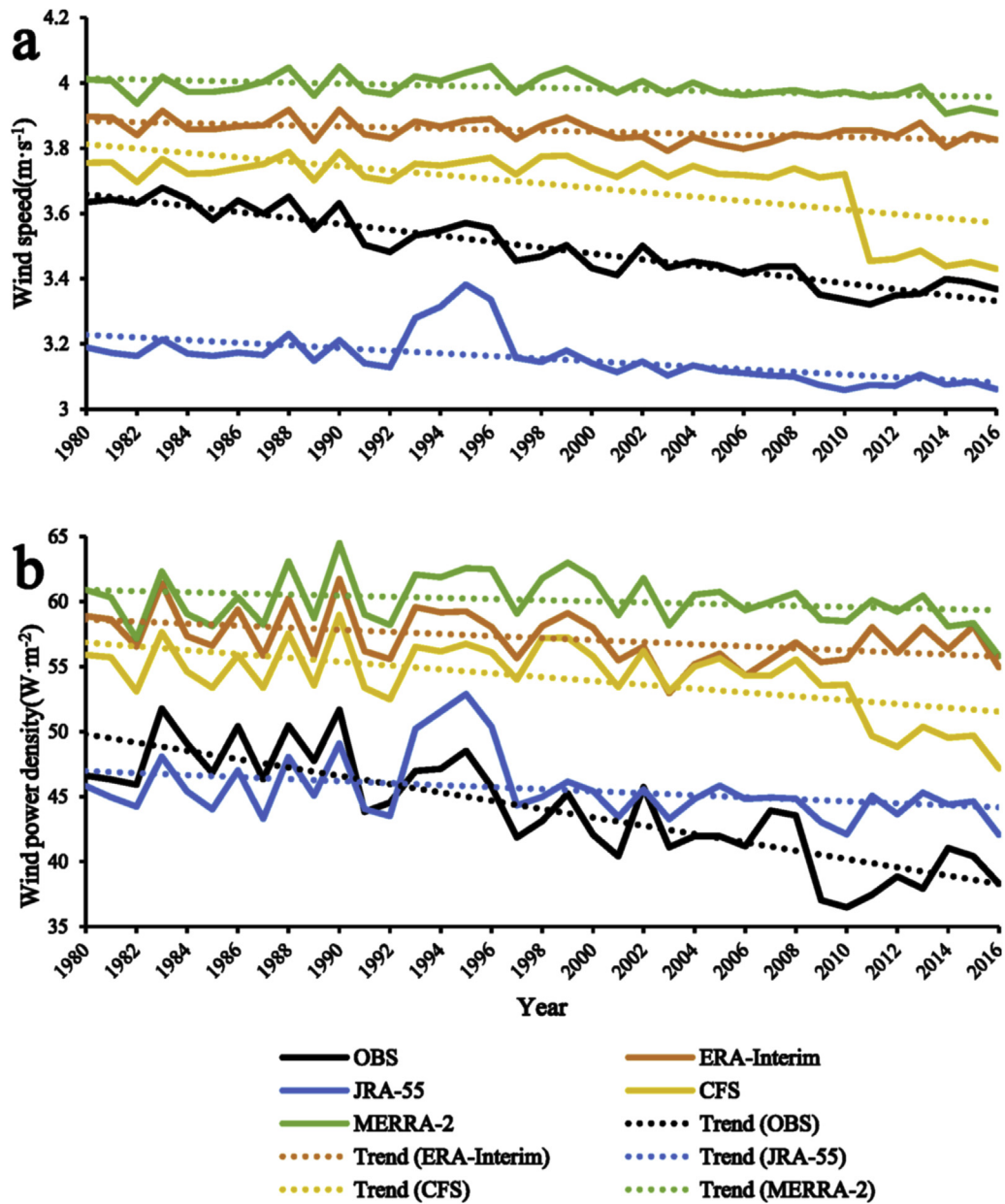
Fig. 2. Time series (*solidline*) and linear trends (*dottedline*) of annual mean wind speeds (**a**, unit: ms^{-1}) and wind power density (**b**, unit: Wm^{-2}) averaged over all stations for the period of 1980−2016. The multi-datasets include OBS (*blackline*), ERA-Interim (*redline*), JRA-55 (*blueline*), CFS (*yellowline*) and MERRA-2 (*greenline*), respectively.

Table 1
Statistical analysis over all stations for the period of 1980−2016, showing correlation coefficient with observations (CC), multiyear mean (MM, ms^{-1}), bias (BIAS, ms^{-1}), root mean square difference (RMSD, ms^{-1}), standard deviation (SD) and linear trend (LT, $ms^{-1}year^{-1}$) of wind speed.

	OBS	ERA-Interim	JRA-55	CFS	MERRA-2
MM	3.495	3.854	3.155	3.692	3.985
BIAS	0	0.359	−0.340	0.197	0.490
RMSD	0	0.370	0.349	0.217	0.499
CC	1	0.608	0.672	0.621	0.523
SD	0.106	0.033	0.076	0.110	0.037
LT	−0.0091	−0.0016	−0.0041	−0.0067	−0.0016

Table 2
Same as Table 1 but for the wind power density (Wm^{-2}).

	OBS	ERA-Interim	JRA-55	CFS	MERRA-2
MM	44.039	57.201	45.571	54.198	60.107
BIAS	0	13.162	1.532	10.159	16.068
RMSD	0	13.559	3.576	10.583	16.455
CC	1	0.636	0.623	0.697	0.515
SD	4.187	1.975	2.523	2.725	1.917
LT	−0.3202	−0.0792	−0.0777	−0.1479	−0.0435

has the best performance of wind speed in terms of climatological characteristics and linear trend based on these statistical indices. MERRA-2 is the least reliable to describe the wind speed averaged

the Northern Hemisphere region. There are also studies to indicate that MERRA has the worst bias ranking of global wind speed, with the comparison of ERA-Interim, CFS and NCEP [65]. For the wind power density (Table 2), results are similar to the wind speed, which JRA-55 and CFS are the closest datasets to the observational

results.

3.2. Seasonal wind speed and wind power density variations

Wind speeds in different seasons have different performances in different reanalysis datasets. The time series and trends of mean seasonal wind speeds and wind power density from all datasets are shown in Figs. 3 and 4, respectively. In general, the climatological characteristics of time series on seasonal and annual mean are similar with significant interannual variability. And the seasonal trends mostly have decreased over the Northern Hemisphere. For the wind speed (Fig. 3), except JRA-55, reanalysis datasets overestimate the values in spring, autumn and winter. In summer, ERA-Interim and MERRA-2 both have closer values with the observations than other datasets, but all of the reanalysis products fail to correctly reflect the trends of wind speeds in autumn. It is worth noting that JRA-55 has the best skill at capturing the variability and trend in winter although it deviates the most from the observations in summer.

For the wind power density (Fig. 4), similar to the wind speed, it also shows downward trends in all four seasons. But not all of the

reanalyses can accurately reproduce the seasonal variability of wind power density. The reanalysis datasets generally underestimate the wind power density in summer and overestimate it in winter, although they can capture the interannual variability in these two seasons. Except for summer, JRA-55 shows more consistency with the observations, and MERRA-2 shows relatively poor performance.

In order to quantify the accuracy of seasonal wind speeds in the reanalysis datasets, the statistics indices analyzed above are calculated, shown in Fig. 5. As demonstrated in Fig. 5 a, seasonal mean wind speeds in summer are slightly lower than winter for all reanalysis products. Statistical results show that JRA-55 performs the best during the cold seasons, while CFS and ERA-Interim have the lowest biases in spring and summer, respectively. Correlation coefficients and standard deviation are used to represent the interannual variabilities of wind speeds and found that JRA-55 and CFS exhibit greater abilities than the other two reanalyses to depict the interannual variability of wind speeds in all four seasons. All reanalysis datasets underestimate the magnitudes of linear trends, especially the ERA-Interim and MERRA-2 datasets, with values close to zero in spring and winter. In addition, the downward trends
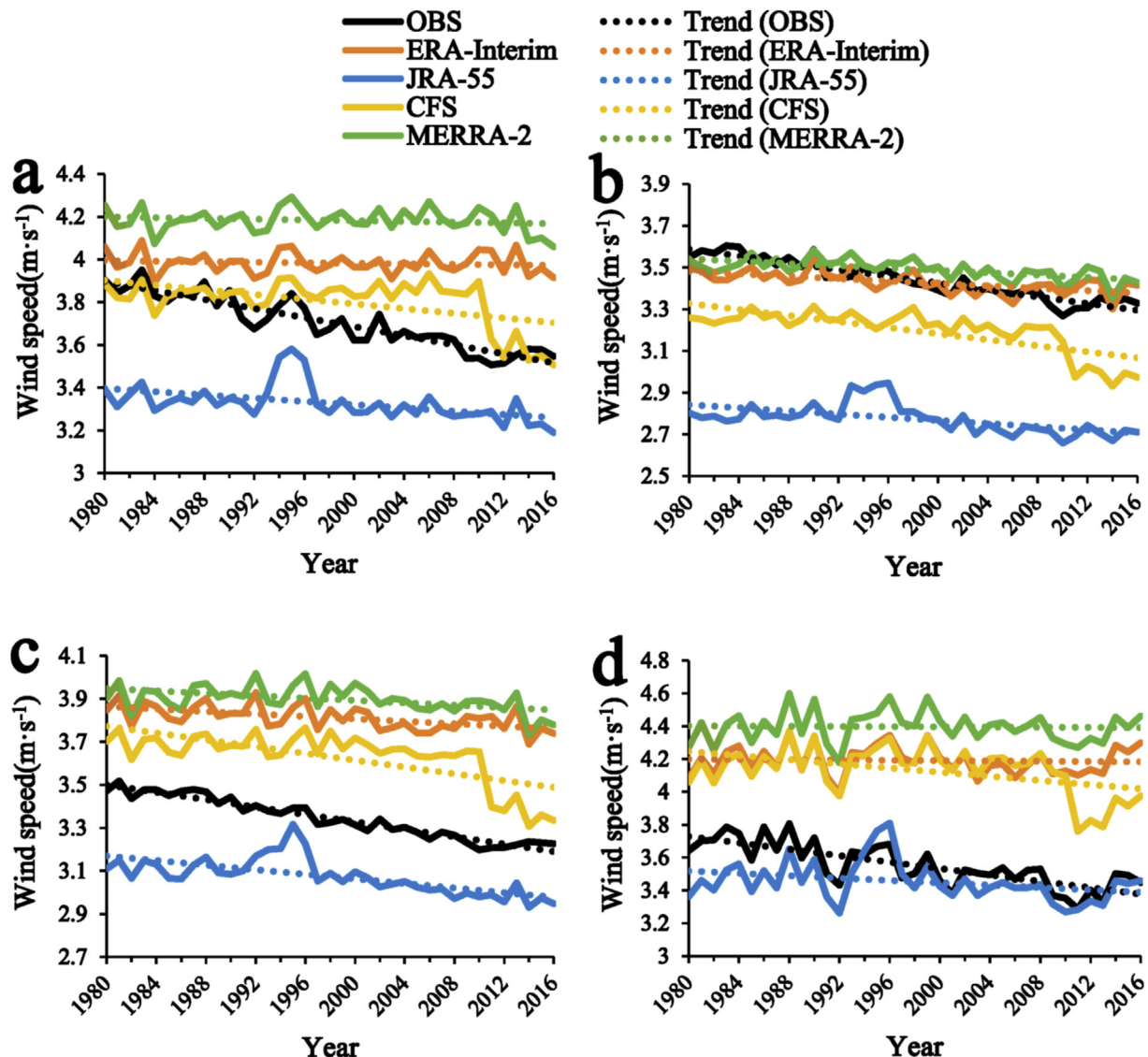

Fig. 3. Same as Fig. 2, but for time series of mean seasonal wind speeds. a-d represent spring, summer, autumn and winter, respectively.
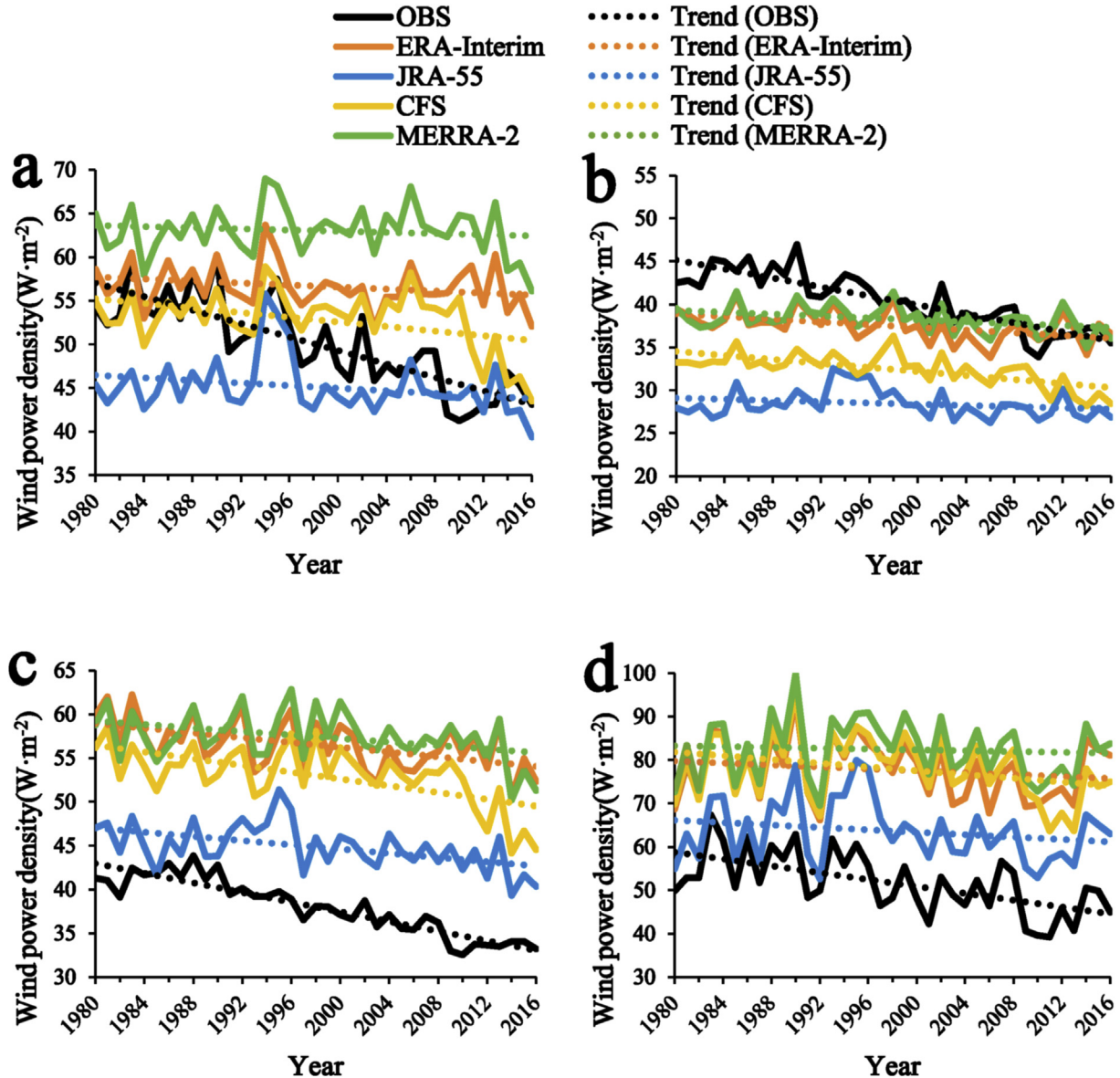
Fig. 4. Same as Fig. 3, but for wind power density.

exhibited by the CFS dataset in all four seasons are closest to the observations. However, MERRA-2 performs even worse than other reanalysis products with higher biases of seasonal mean wind speeds, worst correlation and largest trend deviations from the observations.

The statistical results of wind power density are similar to that in wind speed: seasonal means are maximal in winter and minimal in summer. All of the reanalyses overestimate the wind power density and present larger biases in cold seasons. JRA-55 tends to better reflect the mean seasonal values in cold seasons, while CFS and ERA-Interim are better at representing them in warm seasons. Besides, the interannual wind power density variabilities are accurately reproduced by the CFS dataset in all seasons (Fig. 6d and e) and all datasets perform better in winter than other seasons. In terms of the linear trend, observed values reach about -0.4 $Wm^{-2}year^{-1}$ in spring and winter and about $-0.25 \ Wm^{-2}year^{-1}$ in summer and autumn. However, except for the values of CFS of about $-0.2 \ Wm^{-2}year^{-1}$ in autumn and winter, the values of the other datasets in all four seasons are only between 0 and -0.15

$Wm^{-2}year^{-1}$, which significantly underestimate the trend magnitudes comparing with the observational results.

4. Comparison of multiple datasets in different regions

The spatial distribution of surface wind speeds over three major regions is shown in Fig. 7. It shows obvious regional inconsistencies over the Northern Hemisphere, with the highest value of 4.35 ms^{-1} averaged over North America and the lowest value of 2.75 ms^{-1} averaged over Asia. In Europe, the surface wind speeds decrease gradually from west to east and China has a gradient characteristic of decrease from northeast to southwest, with an average value of less than 4 ms^{-1}. It is worth noting that the climatological mean surface wind speeds at the coastal region get larger values in East Asia.
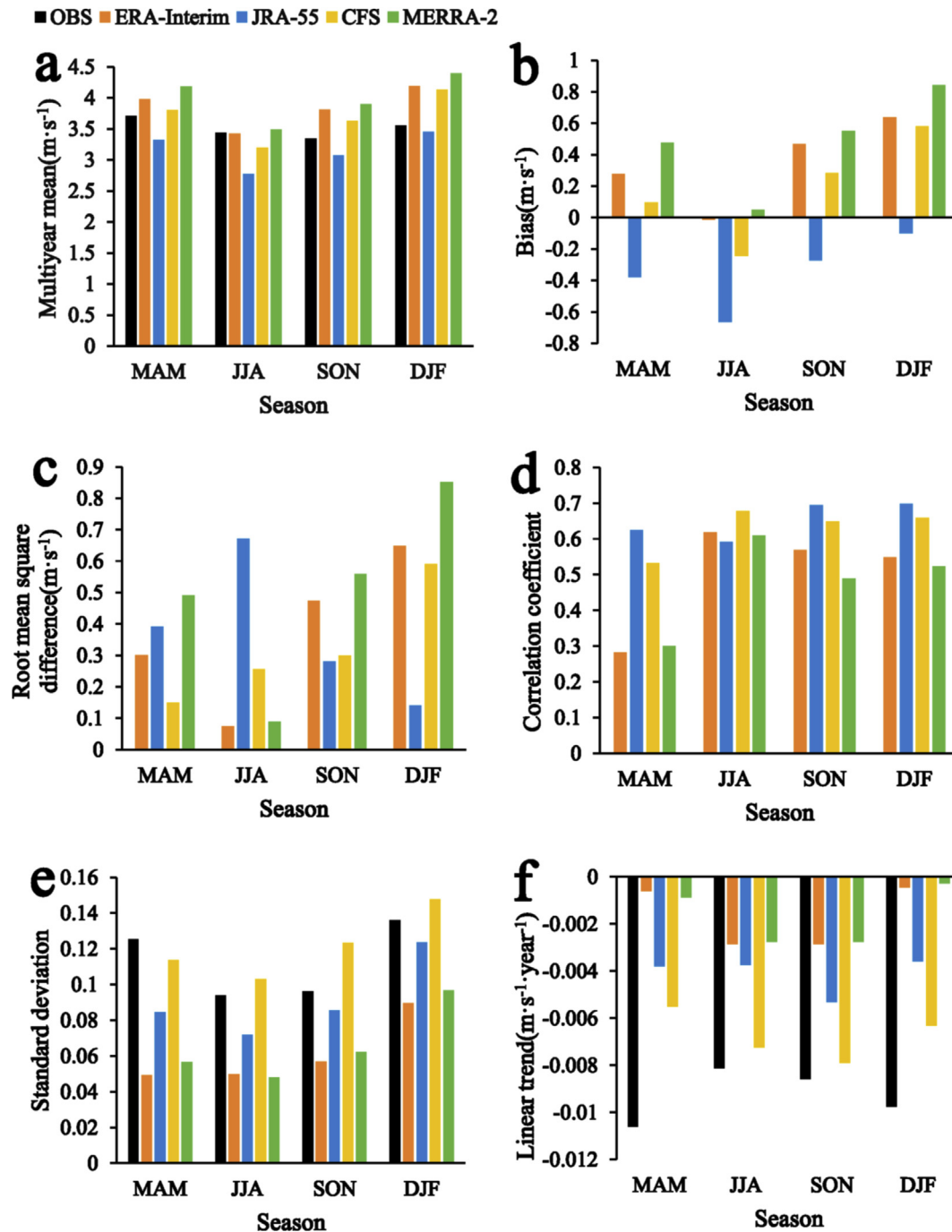
Fig. 5. Magnitudes of seasonal mean wind speed (**a**; unit: ms^{-1}), wind speed bias (**b**; unit: ms^{-1}), root mean square difference (**c**; unit: ms^{-1}), correlation coefficient (**d**), standard deviation (**e**), and linear trend (**f**; unit: $ms^{-1}year^{-1}$) based on the multiple datasets averaged all stations for the period of 1980–2016. MAM, JJA, SON, DJF represent spring, summer, autumn and winter, respectively.

4.1. Comparison of climatological and seasonal differences

Spatial distributions of the percentage differences of wind speeds between the observations and four reanalyses over three regions are compared in Fig. 8. Spatial patterns analyzed by the reanalyses tend to be better represented in Europe, and CFS performs best in Western Europe. The largest discrepancies for these three regions were observed in Asia. It is clear that ERA-Interim, CFS, and MERRA-2 considerably overestimate the wind speed in Asia, and MERRA-2 has the largest positive biases with values of

percentage difference exceeding 90% in most parts. Although JRA-55 also overestimates the climatological means of wind speeds in Japan and northwest China, it shows high consistency with the observations in the rest of Asia. Unlike the spatial patterns in Europe and Asia, there are significant negative biases in most of North America from all products. MERRA-2, which is more consistent with the observations in North America, has a smaller percentage difference at the regional mean of −13.47% than the other three reanalyses except for the southeast coastal regions.

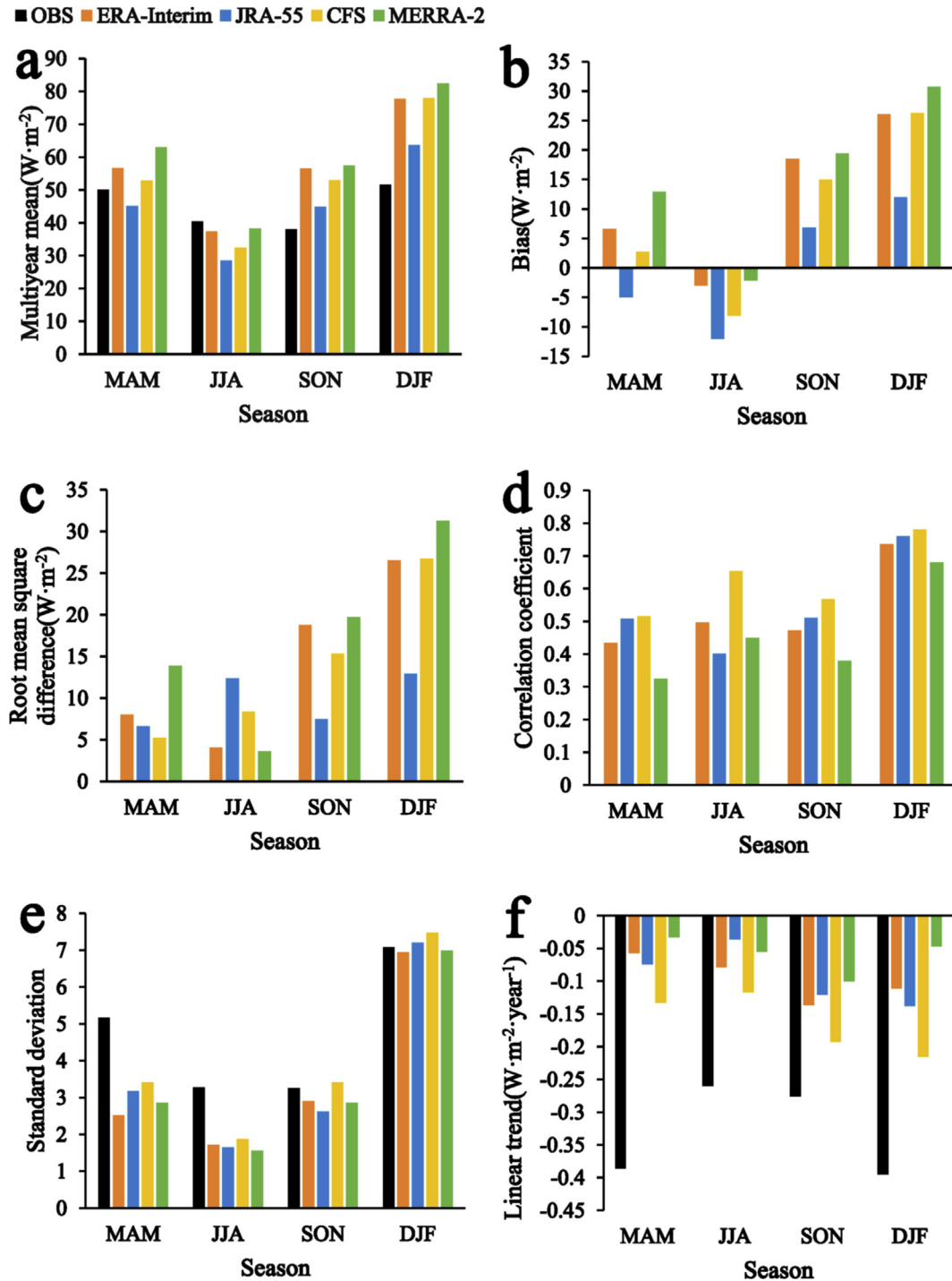Since the wind power density is proportional to the cube of

Fig. 6. Same as Fig. 5, but for the wind power density.

wind speed, the percentage differences of wind power density tend to be larger than wind speed (Fig. 9). The most striking differences from wind speed are in Asia, where the largest percentage differences are over 250% in most of China and coastal regions of Japan based on the ERA-Interim, CFS and MERRA-2. JRA-55 also has the best performance of wind power density with the smallest percentage differences than the other three reanalyses, with around 180% in the coastal regions and western China and −60% in the rest of Asia. In Europe, MERRA-2 and ERA-Interim show positive wind power density biases while negative bias for JRA-55. In particular,

CFS still performs the best in Europe with the smallest regional mean value at 106.7%. In North America, there is no one reanalysis dataset which has obviously better performance on wind power density. Although MERRA-2 performs better in central North America in terms of wind speed, owing to the higher climatological average wind speed in the region, it has a similar performance with the other reanalyses in most of North America at about −60% difference.

Since wind in different regions is dominated by different climate systems in different seasons, the examination of mean annual and
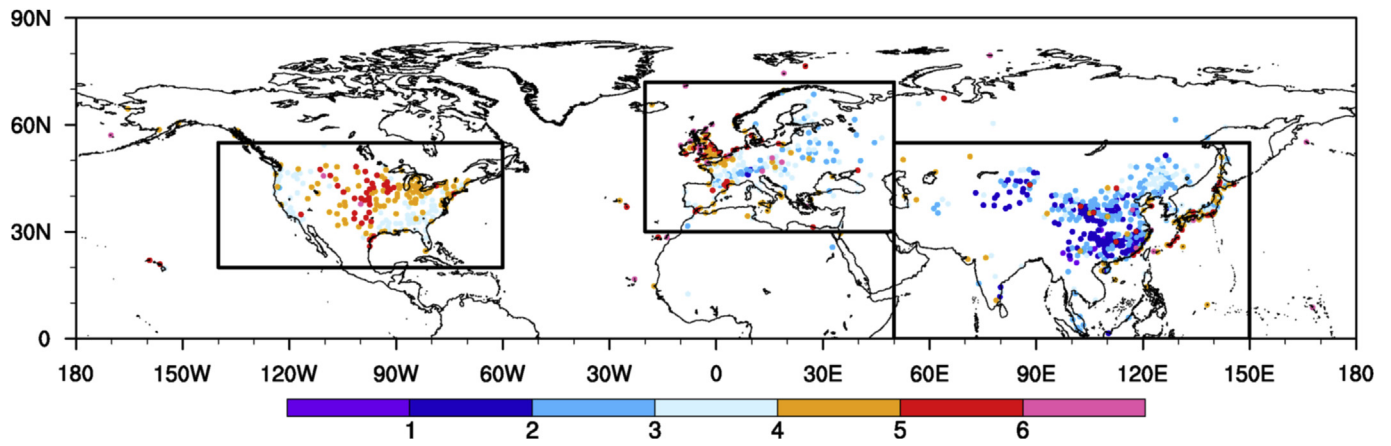
Fig. 7. Spatial distribution of climatological mean surface wind speeds (ms^{-1}) based on observations for the period of 1980−2016. The meteorological stations are represented by dots.
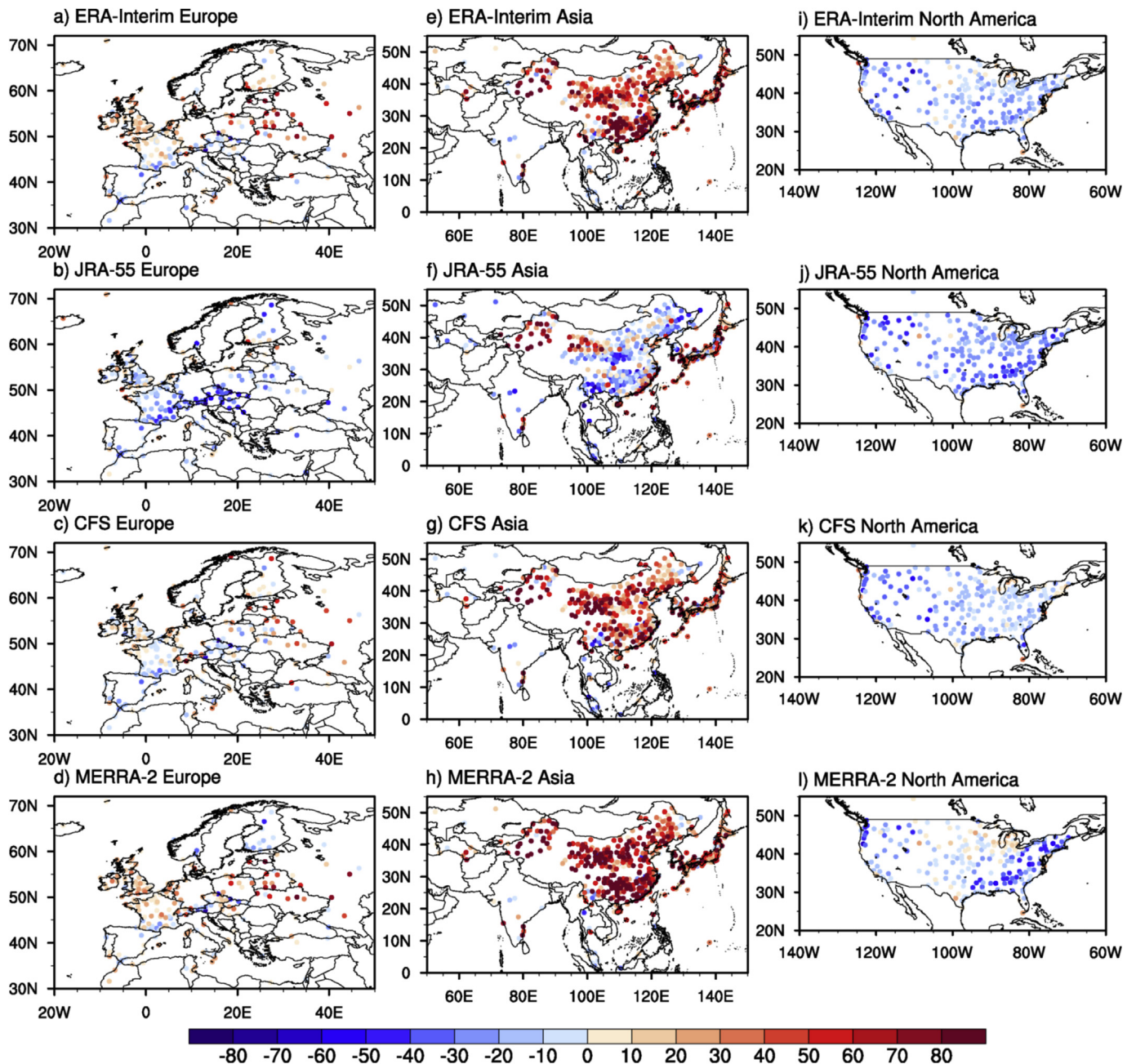

Fig. 8. Spatial distribution of the percentage difference of wind speeds (ms^{-1}) between observational dataset and reanalysis datasets in Europe (**a-d**), Asia (**e-h**) and North America (**i-l**) during 1980−2016 based on the four reanalysis datasets, including ERA-Interim (**a, e** and **i**), JRA-55 (**b, f** and **j**), CFS (**c, g** and **k**) and MERRA-2 (**d, h** and **l**).
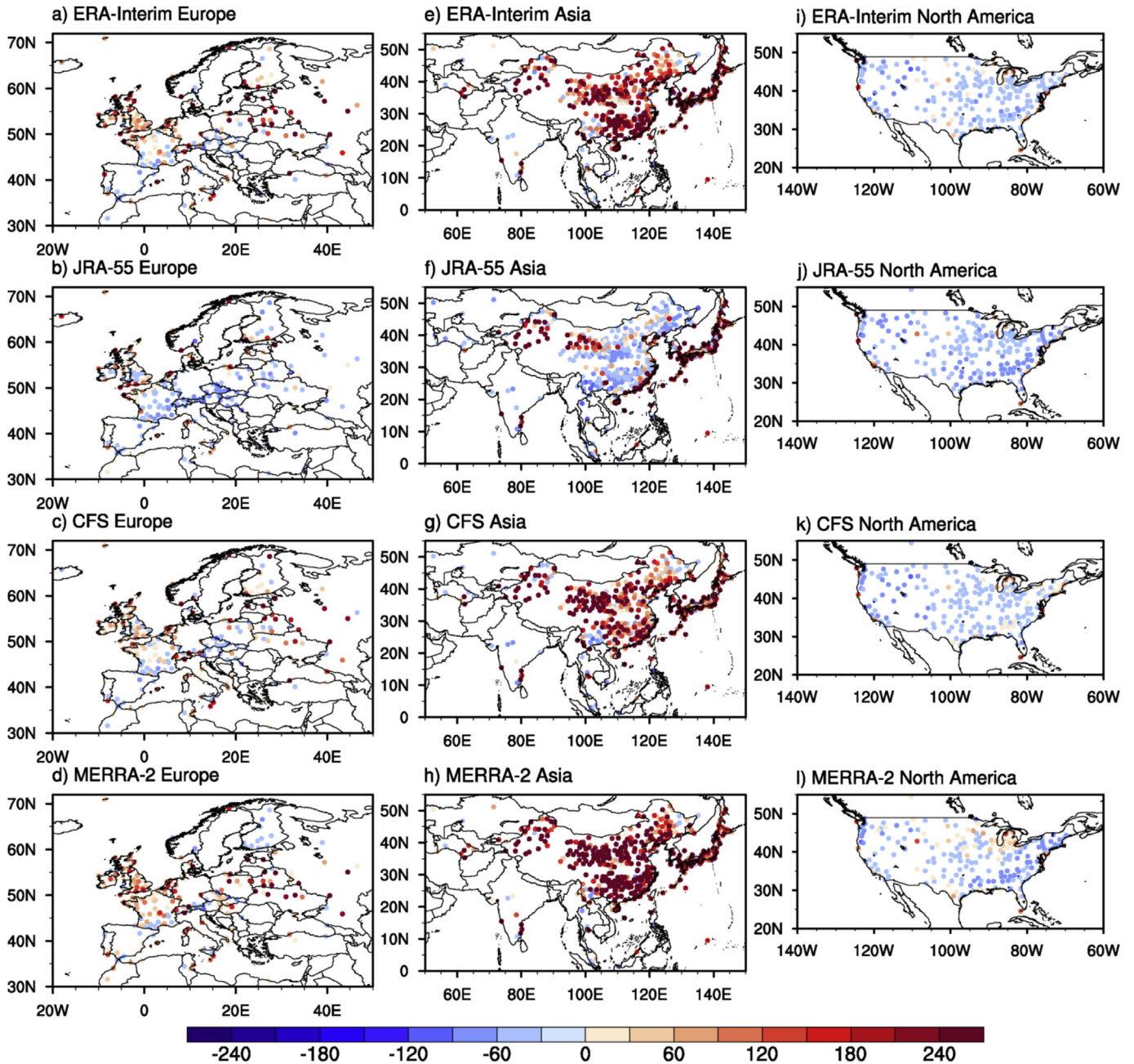
Fig. 9. Same as Fig. 8, but for the wind power density (Wm^{-2}).

seasonal wind speeds and wind power density biases for each region separately may help to give a more detailed assessment of reanalyses quality. In general, these two indicators: wind speed and wind power density have similar characteristics of annual and seasonal mean biases (Fig. 10). Almost all reanalyses underestimate these two indicators in warm seasons and overestimate them in cold seasons in Europe, while show positive bias in Asia and negative bias in North America in all seasons. For the seasonal variability in each region, reanalyses have the best performance in summer and poor performance in winter over the Asia region, while North America is the opposite of Asia with the smallest deviation in winter and the largest in summer. Specifically, in Asia JRA-55 has the best performance in all seasons, with slight positive or negative deviation below 0.25 ms^{-1} in wind speed (Fig. 10c and d). Besides, although MERRA-2 obviously overestimates the wind

speed and wind power density in Asia, it has fewer biases in all seasons in North America compared to the other reanalyses (Fig. 10e and f). In Europe, the reanalysis datasets show significant seasonal differences of wind speed and wind power density. In warm seasons, ERA-Interim and MERRA-2 have fewer biases and JRA-55 shows a large negative bias, while it is the opposite in cold seasons (Fig. 10a and b). Thus, these four reanalysis products have different performances in different seasons on each region.

4.2. Comparison of correlations

The spatial distribution and regional means of correlation coefficients between the observations andfour reanalyses over the different regions are summarized in Fig. 11 and Table 3, respectively. In general, all reanalyses are positively correlated with the
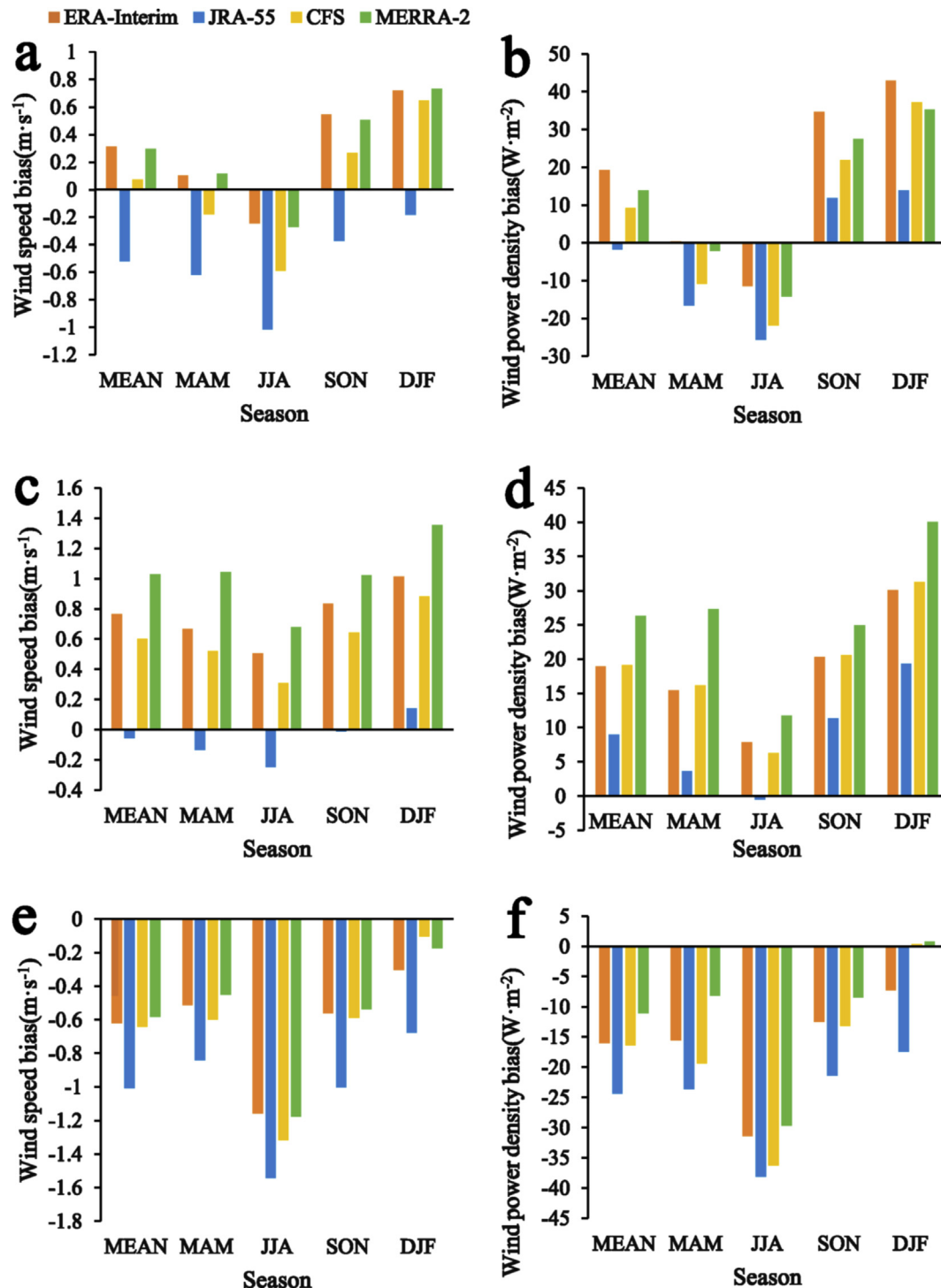
Fig. 10. Biases of annual and seasonal wind speeds (**a, c** and **e**; unit: ms^{-1}) and wind power density (**b, d** and **f**; unit: Wm^{-2}) in different regions. Europe, Asia and North America are shown in **a** and **b**, **c** and **d**, **e** and **f**, respectively.

observed data, except for some stations located in the central and western parts of China. In Europe, the spatial patterns of correlation coefficients by all products are consistent with each other, with the highest correlation of JRA-55 by 0.747.

The correlation coefficients between JRA-55 and observations are the highest in Europe and Asia with the correlations at 0.747 and 0.702 respectively (Table 3). And for these two regions, most spatial correlations generally exceed 0.6 (Fig. 11). Although JRA-55

also has higher spatial correlation coefficients (greater than 0.6) in most of eastern North America, it presents relatively low values in the west (Fig. 11 j). CFS is the second-best performance of correlation with observed, especially presenting North America with the highest regional mean correlation at 0.717. And the spatial patterns of correlation coefficients from all products are consistent with each other in North America, with the highest value in the central part of America. In Asia, the spatial patterns present a positive
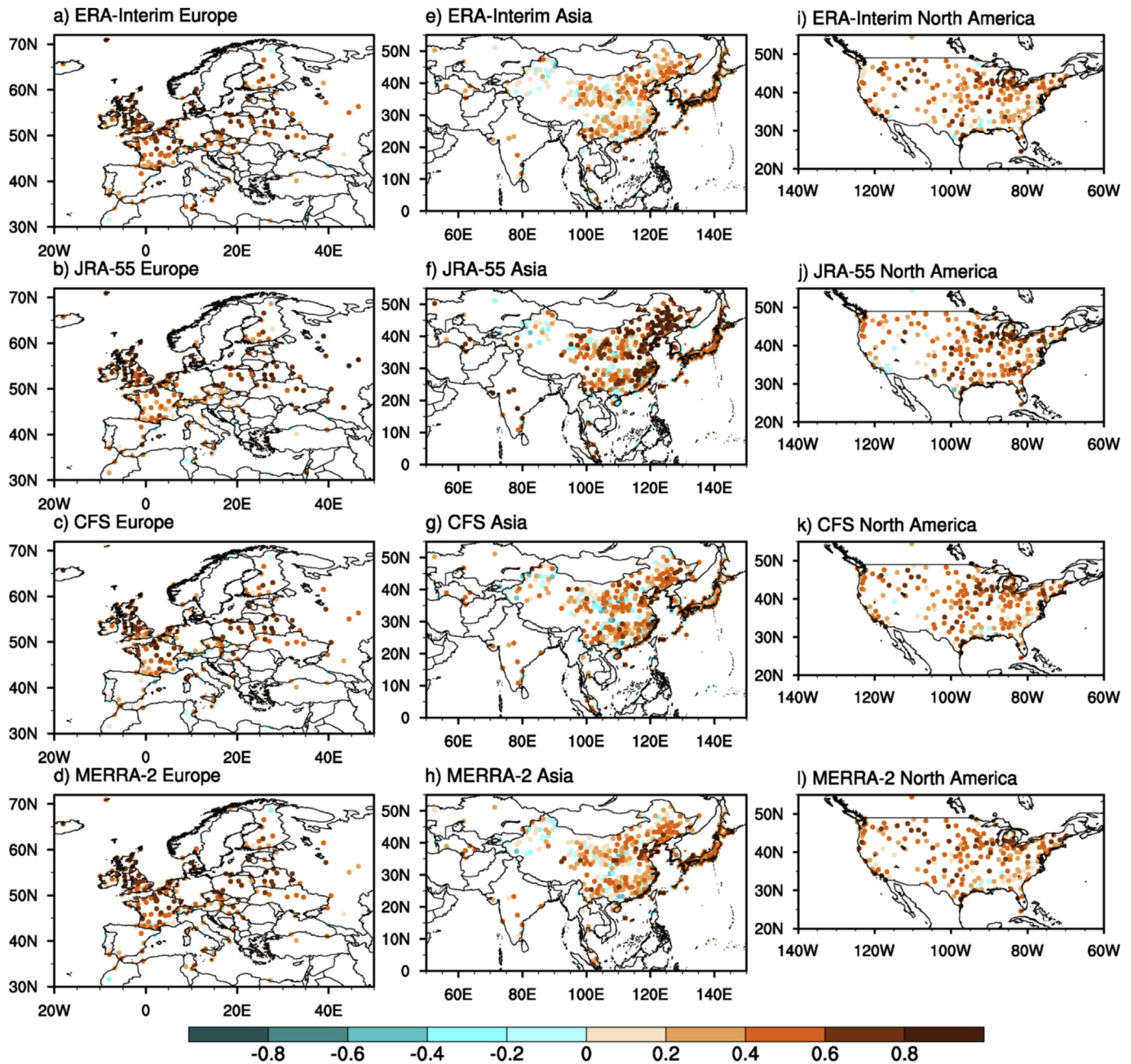
Fig. 11. Spatial distribution of correlation coefficients between the annual mean wind speed from the observational dataset and four reanalyses in Europe (**a-d**), Asia (**e-h**) and North America (**i-l**) during 1980−2016.

Table 3
Correlation coefficients of wind speeds (WS) and wind power density (WPD) between the observational dataset and four reanalyses in different regions.

	Europe		Asia		North America	
	WS	WPD	WS	WPD	WS	WPD
ERA-Interim	0.695	0.788	0.499	0.434	0.651	0.713
JRA-55	0.747	0.840	0.702	0.086	0.590	0.588
CFS	0.602	0.819	0.637	0.609	0.717	0.758
MERRA-2	0.673	0.800	0.524	0.350	0.629	0.665

correlation except for some stations located in the central and western parts of China and coastal regions. Among these four reanalyses, JRA-55 has the highest correlation coefficients in wind

speed and wind power density, especially in the central and northeastern China. Thus, JRA-55 outperforms the other three reanalyses in terms of correlation coefficients in Europe and Asia, and CFS has the highest correlation coefficient in North America. However, ERA-Interim and MERRA-2 present poor accuracy with relatively low correlations in Asia.

4.3. Comparison of time series and trends

Fig. 12 presents the comparisons of the time series of annual mean wind speeds and wind power density based on all products during 1980−2016. These are shown to be similar in most reanalyses to observations in each region. Each of these datasets in different regions shows substantial interannual variability and
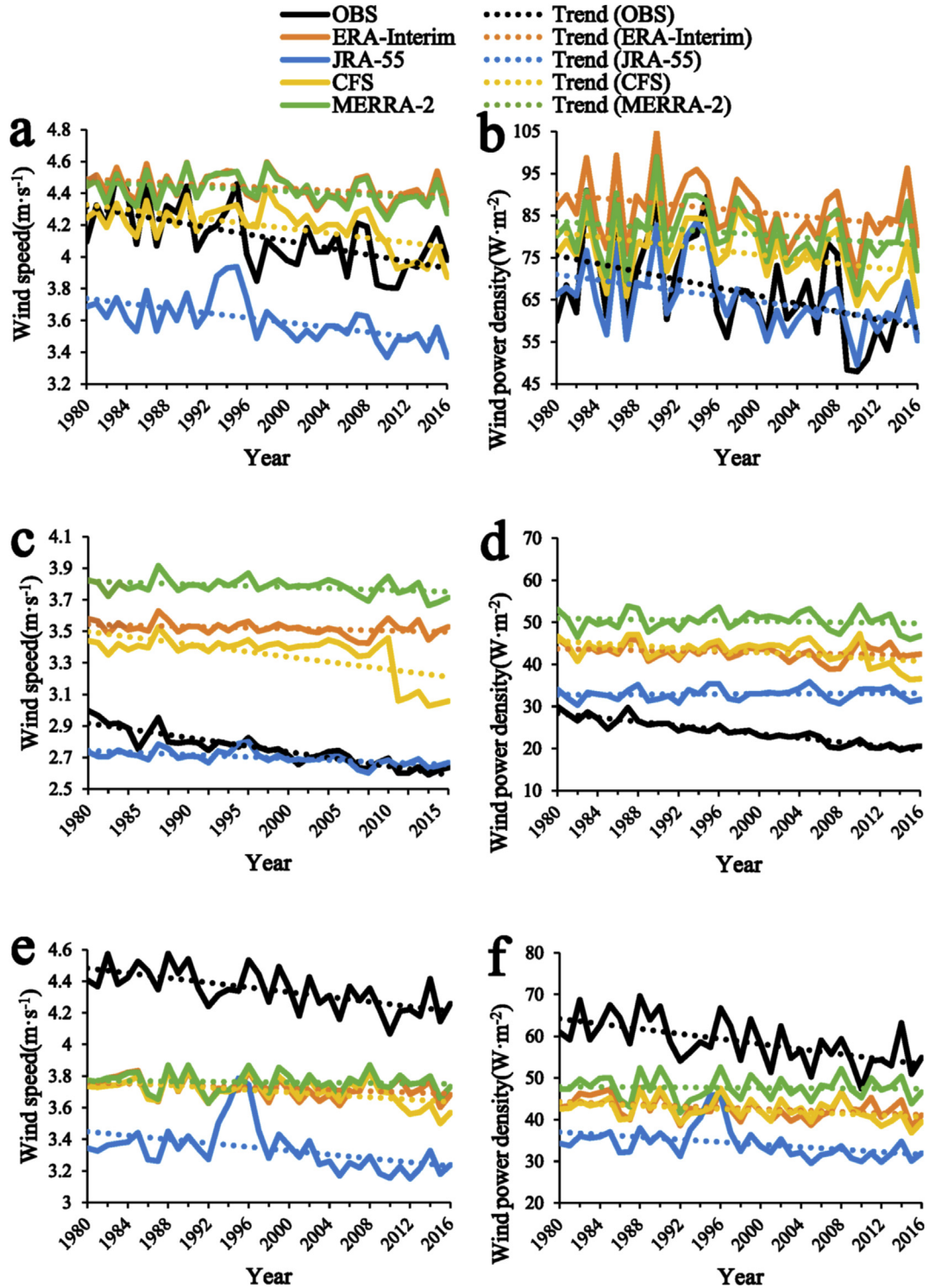
Fig. 12. Time series (*solidline*) and linear trends (*dottedline*) of annual mean wind speeds (ms^{-1}) over **a** Europe, **c** Asia, **e** North America and wind power density (Wm^{-2}) over **b** Europe, **d** Asia, **f** North America averaged over the Northern Hemisphere during 1980−2016. The multi-datasets include OBS (*blackline*), ERA-Interim (*redline*), JRA-55 (*blueline*), CFS (*yellowline*) and MERRA-2 (*greenline*), respectively.

wind power density has a greater magnitude of fluctuations than wind speed. Besides, most of the reanalyses are consistent with the observations, especially for CFS and JRA-55 combining the statistical analysis in Table 3. However, there are many differences between reanalyses and observations. In Europe, CFS cannot reproduce the huge drop in wind speed from 1994 to 1997, leading to the overestimation of wind speed in the next few years (Fig. 12 a). For wind power density in North America, most reanalyses can capture the interannual variability fairly well but not the observed downtrends (Fig. 12 f). Thus, interannual fluctuations are captured well by most products, especially for CFS and JRA-55, even if trends are not.

In order to make a comparison of the reanalyses with the observations on trends, spatial patterns of wind speed trends during 1980−2016 from the observational dataset and four reanalysis datasets are compared in Fig. 13 and the regional mean trends are shown in Table 4. The regional means of wind speed trends according to the observations are all characterized by a decrease in these three regions, and Europe drops fastest during 1980−2016. Besides, all reanalyses tend to underestimate the magnitude of the
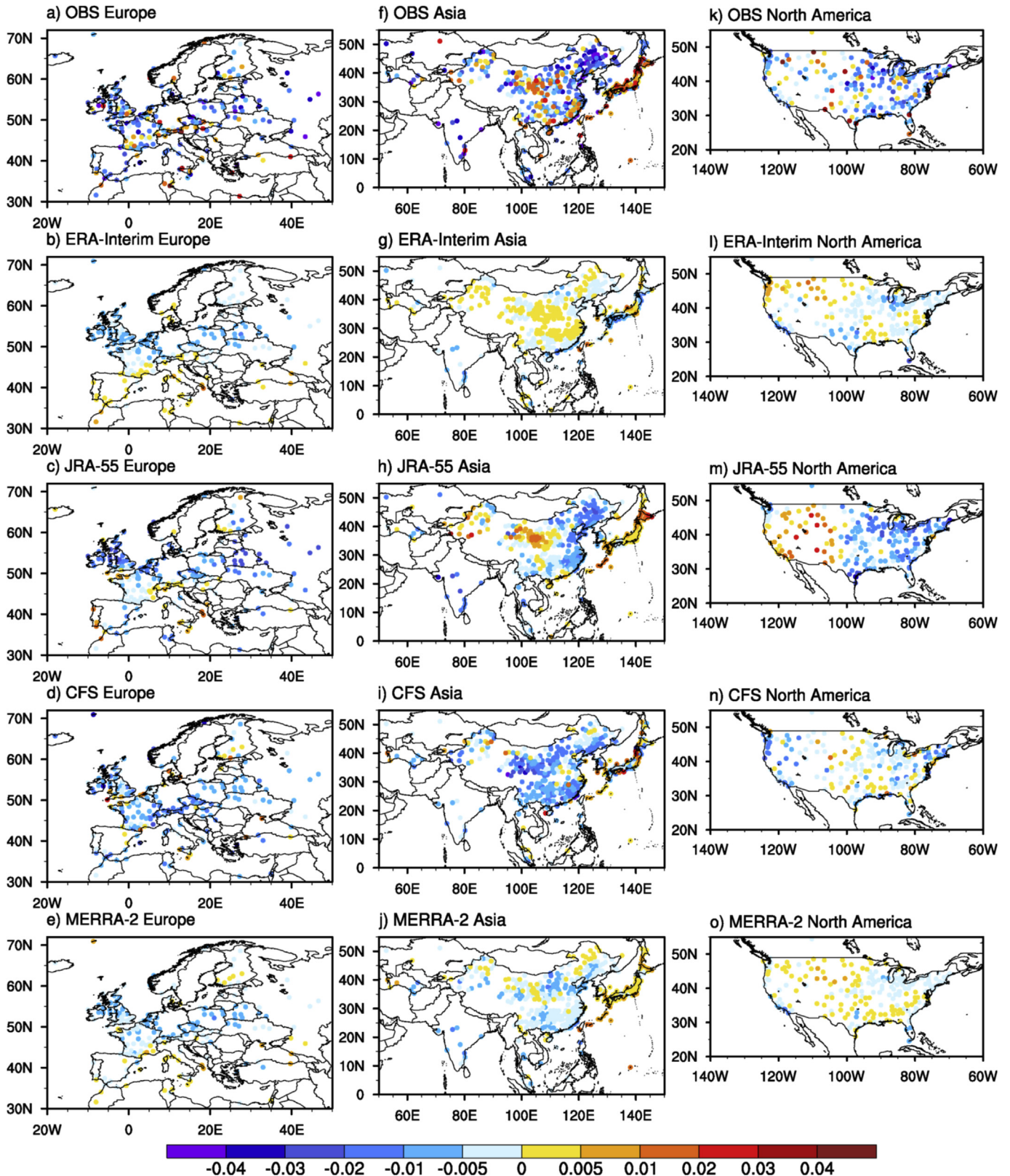

Fig. 13. Spatial distribution of wind speed trends ($ms^{-1}year^{-1}$) in Europe (**a-e**), Asia (**f-j**) and North America (**k-o**) during 1980−2016 based on the observational dataset (**a**, **f** and **k**) and the four reanalysis datasets, including ERA-Interim (**b**, **g** and **l**), JRA-55 (**c**, **h** and **m**), CFS (**d**, **i** and **n**) and MERRA-2 (**e**, **j** and **o**).

Table 4
Wind speed trends $(ms^{-1}year^{-1})$ based on the observational dataset and four reanalyses in different regions.

	Europe	Asia	North America
OBS	−0.0109	−0.0094	−0.0076
ERA-Interim	−0.0030	−0.0013	−0.0020
JRA-55	−0.0075	−0.0025	−0.0060
CFS	−0.0074	−0.0080	−0.0038
MERRA-2	−0.0029	−0.0019	−0.0006

downward trend, especially for ERA-Interim and MERRA-2 with very small magnitudes of the downtrend. Spatially, according to the observations, the decreasing trends of wind speeds occur in most parts of the Northern Hemisphere, except for Central China and the coast of Japan, consistent with previous studies [66]. In general, comparing the results from reanalyses, the pattern is most closely replicated by JRA-55. Through comparing these three regions, all over Europe has a significant downward trend based on the observations and four reanalyses. And the result from JRA-55 with the regional mean of -0.0075 $ms^{-1}year^{-1}$ is the closest to observations, while other reanalyses underestimate the magnitude of trends. In Asia, the spatial characteristics of wind speed trends estimated for JRA-55 lead a similar pattern to those described for observations, with upward trends in Japan and the central-west region of China (Fig. 13 f and h). But JRA-55 underestimates the magnitude of trends since the regional average is only -0.0025 $ms^{-1}year^{-1}$ (Table 4). Based on the observational dataset, there are no obvious spatial distribution features of wind speeds in North America (Fig. 13 k). There are 20.47% of stations with increasing trends as compared to 79.53% of decreasing trends. Spatially, JRA-55 has a good performance of wind speed trends in central and eastern North America and overestimates it in western North America. MERRA-2 gets the largest discrepancy due to it overestimates the magnitude of trends in the central and eastern parts. Overall, both of JRA-55 and CFS can mainly rebuild the spatial patterns of the wind speed trend in Europe and Asia, and JRA-55 is also consistent with the observations in North America, but shows an overestimation in western North America.

5. Discussion

Studying on the variations of surface wind speed and wind power density, especially for the linear trends, has a profound effect on many kinds of application for wind energy. The wind energy industry, one of the biggest user groups of reanalysis datasets, has favored the adoption of reanalyses for assessing wind resources due to the lack of long and homogeneous records of wind speed observations [63,67,68]. This article discusses theoretical wind power resources (i.e. all kinetic energy of air) and the technical detail of wind turbines was not taken into account. Because the available wind observations are temporally averaged values and therefore they are insufficient to consider things like cut-in and cut-off wind speed, which are only reasonable with instant wind speed. The temporally averaged wind speed can reflect a general situation of the wind field, and mathematically, it is the time integration of the wind speed. Assuming the shape of the probability distribution function is the same, a shift in temporal mean wind speed would result in the change of wind power resources that can be utilized by wind turbines, as long as the wind speed is not under cut-in speed or over cut-off speed the whole time (the latter situation is quite impossible over land because of the surface friction). In this sense, the comparison between reanalyses and observations in the present work provides a wide range of reference for the applicability of

the reanalysis data in a certain area or a certain period in order to provide a reference for the selection of wind farm locations in a certain area in further research, which is of great value to wind energy sector.

In this study, the magnitudes of regional mean trends based on different datasets have been displayed in Table 1 for the Northern Hemisphere and Table 4 for these three regions. The surface wind speeds from all observational and reanalysis products have significant decreasing trends. There are several studies to identify the potential drivers of wind speed trend, such as changes in the surface roughness associated with modifications in land use [69−71] or aerosol concentrations [66,70]. These drivers of wind speed trend cannot be the only explanation of the negative trends because they are dealt with in different ways by each reanalysis product and strongly depend on the region selected. An alternative explanation, which is regarded as a primary source of wind speed change, is about the changes in the large-scale circulation [19,66,69,72−75]. Torralba et al. [2] found there is a strong similarity between the trends in 850 hPa and 10 m levels, which illustrates a large part of the trends in 10 m wind can be attributed to the change of atmospheric circulation, in particular the recent strengthening of the Walker circulation [75,76].

Besides, it is worth noting that there are some considerable differences of declining trends among these four reanalysis products over the different regions. In particular, the most significant disagreements are encountered between JRA-55 and MERRA-2. It has been previously discussed that JRA-55 produces more intense regional values of surface wind speed trends than MERRA-2. For the Northern Hemisphere, the trend of surface wind speed from JRA-55 gets -0.0041 $ms^{-1}year^{-1}$, while MERRA-2 just gets -0.0016 $ms^{-1}year^{-1}$ (Table 1). This discrepancy has the largest value over North America, which the magnitude of wind speed trend from JRA-55 is ten times that of MERRA-2 (Table 4). The definitive causes for the differences of wind speed trends among different reanalyses are currently unidentified. However, several hypotheses have been proposed to explain the discrepancy by some studies. Some studies indicate that the trends of surface wind speed provided by reanalysis products are affected by different methods that different reanalyses use to infer 10 m wind speed. For example, the different methodologies from the lowest model level which reanalyses use would have an influence on the inference of 10 m wind [34,65]. For the MERRA-2, the wind speed at 10 m is interpolated with the Helfand and Schubert scheme under the Monin-Obhukhov similarity theory which takes the effects of a viscous sublayer for heat and moisture transport over all surfaces except land into account [61,77]. JRA-55 estimates the 10 m wind speed by using a univariate two-dimensional optimal interpolation process based on the assumption of neutral stability from the lowest model level to reduce the wind speed values in the interpolation from there down to 10 m. The most important difference for inferring the 10 m wind speed is that JRA-55 derives surface wind using neutral stability while MERRA-2 is considering stability-dependent approaches, which could lead to the differences of wind speed trends among different reanalyses [2]. Besides, the spatial resolution also can have an impact on wind speed. The reanalysis models with relatively low spatial resolution would smooth the local terrain features leading to the enhancement of wind speed, which means that the reanalyses are likely to overestimate the wind speed at a particular location [34]. And the observations and assimilation systems used in the different reanalysis products are also the sources of uncertainty affecting these products [2,78]. For example, the wind speed from reanalyses with negative bias may not be fully corrected by the data-assimilation process.

In different reanalysis products, the discrepancies of wind speed

trends may lead to inconsistency of the evaluation of long-term wind power and wind energy resource estimations. The inter-comparison of this study can be helpful to the characterization of the limitations of reanalysis products and to assess the potential of climate predictions, which further contributes to producing more accurate and reliable information for developing strategies of wind energy resource estimation and making a financial decision.

6. Conclusion

Wind energy scientific community oftentimes relies on reanalysis datasets for different activities such as the assessment of the wind energy resources in a particular region due to the lack of long and homogeneous records of surface wind speed from observations. The present work aims to shed light on the differences of wind speed and wind power density between reanalysis products and observations to help the reanalysis users to make decisions about the suitability of a reanalysis dataset over the whole Northern Hemisphere region and different regions there. In this study, four of the most reputable reanalysis datasets including ERA-Interim, JRA-55, CFS, and MERRA-2 are selected to compare with observational references in terms of climatological mean, interannual variability and linear trend. Some important conclusions are as follows.

Over the Northern Hemisphere, only JRA-55 underestimates the climatological means of wind speeds with the mean bias of -0.345 ms^{-1}, while biases of ERA-Interim, CFS and MERRA-2 are higher than the observations. Compared with other reanalyses, the climatological means of wind speeds in CFS are closer to those in observations, and for wind power density JRA-55 is the most relevant to the observations. Besides, the interannual fluctuations are captured well by most datasets, even if they have a tendency to underestimate the variability of wind speeds. JRA-55 and CFS are more similar to observed to have distinct declining trend for the period of 1980−2016 over the Northern Hemisphere even though all reanalyses underestimate the degrees of the wind speed and wind power density decline. From the seasonal point of view, wind speed and wind power density perform similarly, showing significant interannual variability and downward trends in all seasons. ERA-Interim and CFS are consistent with the observations only in summer, while they have huge positive biases in the other three seasons. Reanalyses underestimate the two variables in summer while overestimate them in winter, with the best performance of JRA-55 and CFS and relatively poor performance of MERRA-2.

Furthermore, for three regions: North America, Asia and Europe, the wind speed in North America is significantly higher than that in Asia in terms of climatological mean. All reanalyses underestimate the wind speed in North America, with the best performance of MERRA-2 analyzing the central part of North America. In Asia, JRA-55 is significantly superior to other datasets. The CFS dataset is better matched with the observations in Western Europe, while JRA-55 is better in Eastern Europe. The spatial distribution of correlation coefficients and the evolution of wind speed and wind power density confirm the excellence of the JRA-55 dataset in Asia and Europe, especially for the cold seasons.

All in all, based on multiple evaluations at different temporal and spatial scales, JRA-55 and CFS offer the best estimates of annual mean and seasonal mean wind speeds, interannual variabilities and linear trends over the Northern Hemisphere. The spatial distribution of wind speed trends in Europe and Asia has been well reproduced by the JRA-55 dataset, albeit on a smaller magnitude. But for North America, none of the datasets has this capability. Indeed, there are disagreements in the representation of surface wind speed after analyzing these four reanalysis products, which demonstrates the unavoidable uncertainty affecting these datasets.

Wind energy is currently the most commercial and rapidly developing renewable energy resource. This research may have important economic significance, because understanding the discrepancies of surface wind speed and wind power density variabilities is useful for appropriate risk estimation of wind energy resources and as guidance for the development of policies favoring sustainable adaption initiatives that avoid poor investment decisions.

Declaration of competing interests

The authors declare that they have no known competing financial interests or personal relationships that could have appeared to influence the work reported in this paper.

CRediT authorship contribution statement

Haozeyu Miao: Writing - original draft, Software, Validation, Formal analysis, Investigation. **Danhong Dong:** Methodology, Software, Writing - review & editing. **Gang Huang:** Conceptualization, Supervision, Funding acquisition. **Kaiming Hu:** Writing - review & editing. **Qun Tian:** Software, Writing - review & editing. **Yuanfa Gong:** Supervision.

Acknowledgement

References

[1] Saidur R, Islam M, Rahim N, Solangi K. A review on global wind energy policy. Renew Sustain Energy Rev 2010;14(7):1744−62.
[2] Torralba V, Doblas-Reyes FJ, Gonzalez-Reviriego N. Uncertainty in recent near-surface wind speed trends: a global reanalysis intercomparison. Environ Res Lett 2017;12(11):114019.
[3] Zheng CW, Li CY, Pan J, Liu MY, Xia LL. An overview of global ocean wind energy resource evaluations. Renew Sustain Energy Rev 2016;53:1240−51.
[4] W. P. C. W. Reaches, 597 gw, 50, 1 gw added in. 2018.
[5] Al-Abbadi NM. Wind energy resource assessment for five locations in Saudi Arabia. Renew Energy 2005;30(10):1489−99.
[6] Manwell JF, McGowan JG, Rogers AL. Wind energy explained: theory, design and application. John Wiley & Sons; 2010.
[7] Pryor SC, Barthelmie R. Climate change impacts on wind energy: a review. Renew Sustain Energy Rev 2010;14(1):430−7.
[8] Fyrippis I, Axaopoulos PJ, Panayiotou G. Wind energy potential assessment in naxos island, Greece. Appl Energy 2010;87(2):577−86.
[9] Rehman S, Mahbub Alam A, Meyer JP, Al-Hadhrami L. Wind speed characteristics and resource assessment using weibull parameters. Int J Green Energy 2012;9(8):800−14.
[10] Wu J, Wang J, Chi D. Wind energy potential assessment for the site of inner Mongolia in China. Renew Sustain Energy Rev 2013;21:215−28.
[11] Baseer MA, Meyer JP, Rehman S, Alam MM. Wind power characteristics of

seven data collection sites in jubail, Saudi Arabia using weibull parameters. Renew Energy 2017;102:35–49.

[12] Hulio ZH, Jiang W, Rehman S. Techno-economic assessment of wind power potential of hawke's bay using weibull parameter: a review. Energy Strat.Rev. 2019;26:100375.

[13] Young I, Zieger S, Babanin AV. Global trends in wind speed and wave height. Science 2011;332(6028):451–5.

[14] Tian Q, Huang G, Hu K, Niyogi D. Observed and global climate model based changes in wind power potential over the northern hemisphere during 1979–2016. Energy 2019;167:1224–35.

[15] Pryor S, Barthelmie R, Riley E. Historical evolution of wind climates in the USA. In: Journal of physics: conference series, vol. 75. IOP Publishing; 2007. 012065.

[16] McVicar TR, Van Niel TG, Li LT, Roderick ML, Rayner DP, Ricciardulli L, Donohue RJ. Wind speed climatology and trends for Australia, 1975–2006: capturing the stilling phenomenon and comparison with near-surface reanalysis output. Geophys Res Lett 2008;35(20).

[17] Wan H, Wang XL, Swail VR. Homogenization and trend analysis of canadian near-surface wind speeds. J Clim 2010;23(5):1209–25.

[18] Minquan X. Climate regionalization and characteristics of surface winds over China in recent 30 years. Plateau Meteorol 2015;34(1):39–49.

[19] Azorin-Molina C, Rehman S, Guijarro JA, McVicar TR, Minola L, Chen D, Vicente-Serrano SM. Recent trends in wind speed across Saudi Arabia, 1978–2013: a break in the stilling. Int J Climatol 2018;38:e966–84.

[20] Rehman S. Long-term wind speed analysis and detection of its trends using mann–kendall test and linear regression method. Arabian J Sci Eng 2013;38(2):421–37.

[21] Himri Y, Rehman S, Himri S, Mohammadi K, Sahin B, Malik AS. Investigation of wind resources in timimoun region, Algeria. Wind Eng 2016;40(3):250–60.

[22] McVicar TR, Roderick ML, Donohue RJ, Li LT, Van Niel TG, Thomas A, Grieser J, Jhajharia D, Himri Y, Mahowald NM, et al. Global review and synthesis of trends in observed terrestrial near-surface wind speeds: implications for evaporation. J Hydrol 2012;416:182–205.

[23] Lin C, Yang K, Huang J, Tang W, Qin J, Niu X, Chen Y, Chen D, Lu N, Fu R. Impacts of wind stilling on solar radiation variability in China. Sci Rep 2015;5: 15135.

[24] Archer CL, Jacobson MZ. Evaluation of global wind power. J Geophys Res: Atmos. 2005;110(D12).

[25] Pryor S, Barthelmie R. Assessing climate change impacts on the near-term stability of the wind energy resource over the United States. Proc Natl Acad Sci Unit States Am 2011;108(20):8167–71.

[26] Zhou Y, Luckow P, Smith SJ, Clarke L. Evaluation of global onshore wind energy potential and generation costs. Environ Sci Technol 2012;46(14): 7857–64.

[27] Onea F, Rusu E. An evaluation of the wind energy in the north-west of the black sea. Int J Green Energy 2014;11(5):465–87.

[28] Pryor S, Barthelmie R, Kjellström E. Potential climate change impact on wind energy resources in northern europe: analyses using a regional climate model. Clim Dynam 2005;25(7–8):815–35.

[29] Pryor S, Schoof J, Barthelmie R. Climate change impacts on wind speeds and wind energy density in northern europe: empirical downscaling of multiple aogcms. Clim Res 2005;29(3):183–98.

[30] Shi J, Qu X, Zeng S. Short-term wind power generation forecasting: direct versus indirect arima-based approaches. Int J Green Energy 2011;8(1): 100–12.

[31] Hueging H, Haas R, Born K, Jacob D, Pinto JG. Regional changes in wind energy potential over europe using regional climate model ensemble projections. J. Appl. Meteorol. Clim. 2013;52(4):903–17.

[32] Reyers M, Moemken J, Pinto JG. Future changes of wind energy potentials over europe in a large cmip5 multi-model ensemble. Int J Climatol 2016;36(2): 783–96.

[33] Aristidi E, Agabi K, Azouit M, Fossat E, Vernin J, Travouillon T, Lawrence J, Meyer C, Storey J, Halter B, et al. An analysis of temperatures and wind speeds above dome c, Antarctica. Astron Astrophys 2005;430(2):739–46.

[34] Rose S, Apt J. What can reanalysis data tell us about wind power? Renew Energy 2015;83:963–9.

[35] Marcos R, González-Reviriego N, Torralba V, Soret A, Doblas-Reyes FJ. Characterization of the near surface wind speed distribution at global scale: era-interim reanalysis and ecmwf seasonal forecasting system 4. Clim Dynam 2019;52(5–6):3307–19.

[36] Hagspiel S, Papaemannouil A, Schmid M, Andersson G. Copula-based modeling of stochastic wind power in europe and implications for the swiss power grid. Appl Energy 2012;96:33–44.

[37] Kubik M, Brayshaw DJ, Coker PJ, Barlow JF. Exploring the role of reanalysis data in simulating regional wind generation variability over northern Ireland. Renew Energy 2013;57:558–61.

[38] Olauson J, Bergkvist M. Modelling the Swedish wind power production using merra reanalysis data. Renew Energy 2015;76:717–25.

[39] Li H, Robock A, Liu S, Mo X, Viterbo P. Evaluation of reanalysis soil moisture simulations using updated Chinese soil moisture observations. J Hydrometeorol 2005;6(2):180–93.

[40] Khan V, Holko L, Rubinstein K, Breiling M. Snow cover characteristics over the main Russian river basins as represented by reanalyses and measured data. J. Appl. Meteorol. Clim. 2008;47(6):1819–33.

[41] Bao X, Zhang F. Evaluation of ncep–cfsr, ncep–ncar, era-interim, and era-40 reanalysis datasets against independent sounding observations over the Tibetan plateau. J Clim 2013;26(1):206–14.

[42] Pfeifroth U, Mueller R, Ahrens B. Evaluation of satellite-based and reanalysis precipitation data in the tropical pacific. J. Appl. Meteorol. Clim. 2013;52(3): 634–44.

[43] Jones R, Renfrew I, Orr A, Webber B, Holland D, Lazzara M. Evaluation of four global reanalysis products using in situ observations in the amundsen sea embayment, Antarctica. J Geophys Res: Atmos. 2016;121(11):6240–57.

[44] Yang K, Zhang J. Evaluation of reanalysis datasets against observational soil temperature data over China. Clim Dynam 2018;50(1–2):317–37.

[45] Simmons A, Jones P, da Costa Bechtold V, Beljaars A, Kållberg P, Saarinen S, Uppala S, Viterbo P, Wedi N. Comparison of trends and low-frequency variability in cru, era-40, and ncep/ncar analyses of surface air temperature. J Geophys Res: Atmos. 2004;109(D24).

[46] Makshtas A, Atkinson D, Kulakov M, Shutilin S, Krishfield R, Proshutinsky A. Atmospheric forcing validation for modeling the central arctic. Geophys Res Lett 2007;34(20).

[47] Ma L, Zhang T, Li Q, Frauenfeld OW, Qin D. Evaluation of era-40, ncep-1, and ncep-2 reanalysis air temperatures with ground-based measurements in China. J Geophys Res: Atmos. 2008;113(D15).

[48] Mao J, Shi X, Ma L, Kaiser DP, Li Q, Thornton PE. Assessment of reanalysis daily extreme temperatures with China's homogenized historical dataset during 1979–2001 using probability density functions. J Clim 2010;23(24):6605–23.

[49] Zhao J, Xu H. Comparison of wind velocity among reanalysis and radiosone datasets over China [j]. Climat. Environ Res 2014;19(5):587–600.

[50] Kim H-G, Kim J-Y, Kang Y-H. Comparative evaluation of the third-generation reanalysis data for wind resource assessment of the southwestern offshore in South Korea. Atmosphere 2018;9(2):73.

[51] Sterl A, Bakker AM, van den Brink HW, Haarsma R, Stepek A, Wijnant IL, de Winter RC. Large-scale winds in the southern north sea region: the wind part of the knmi'14 climate change scenarios. Environ Res Lett 2015;10(3):035004.

[52] Zahedi A. Current status and future prospects of the wind energy. In: 2012 10th international power & energy conference (IPEC). IEEE; 2012. p. 54–8.

[53] Smith A, Lott N, Vose R. The integrated surface database: recent developments and partnerships. Bull Am Meteorol Soc 2011;92(6):704–8.

[54] Dee DP, Uppala S, Simmons A, Berrisford P, Poli P, Kobayashi S, Andrae U, Balmaseda M, Balsamo G, Bauer dP, et al. The era-interim reanalysis: configuration and performance of the data assimilation system. Q J R Meteorol Soc 2011;137(656):553–97.

[55] Ebita A, Kobayashi S, Ota Y, Moriya M, Kumabe R, Onogi K, Harada Y, Yasui S, Miyaoka K, Takahashi K, et al. The Japanese 55-year reanalysis "jra-55": an interim report. Sola 2011;7:149–52.

[56] Onogi K, Tsutsui J, Koide H, Sakamoto M, Kobayashi S, Hatsushika H, Matsumoto T, Yamazaki N, Kamahori H, Takahashi K, et al. The jra-25 reanalysis. J Meteorol Soc Japan Ser. II 2007;85(3):369–432.

[57] Saha S, Moorthi S, Pan H-L, Wu X, Wang J, Nadiga S, Tripp P, Kistler R, Woollen J, Behringer D, et al. The ncep climate forecast system reanalysis. Bull Am Meteorol Soc 2010;91(8):1015–58.

[58] M. Bosilovich, R. Lucchesi, M. Suarez, Merra-2: file specification.

[59] Rienecker MM, Suarez MJ, Gelaro R, Todling R, Bacmeister J, Liu E, Bosilovich MG, Schubert SD, Takacs L, Kim G-K, et al. Merra: nasa's modern-era retrospective analysis for research and applications. J Clim 2011;24(14): 3624–48.

[60] M. M. Rienecker, M. Suarez, R. Todling, J. Bacmeister, L. Takacs, H. Liu, W. Gu, M. Sienkiewicz, R. Koster, R. Gelaro, et al., The geos-5 data assimilation system: documentation of versions 5.0. 1, 5.1. 0, and 5.2. 0.

[61] Molod A, Takacs L, Suarez M, Bacmeister J. Development of the geos-5 atmospheric general circulation model: evolution from merra to merra2. Geosci Model Dev (GMD) 2015;8(5):1339–56.

[62] Wu W-S, Purser RJ, Parrish DF. Three-dimensional variational analysis with spatially inhomogeneous covariances. Mon Weather Rev 2002;130(12): 2905–16.

[63] Cannon DJ, Brayshaw DJ, Methven J, Coker PJ, Lenaghan D. Using reanalysis data to quantify extreme wind power generation statistics: a 33 year case study in great britain. Renew Energy 2015;75:767–78.

[64] Kvasov R, Cruz-Pol S, Colom-Ustáriz J, Colón LL, Rees P. Weather radar data visualization using first-order interpolation. In: 2013 IEEE international geoscience and remote sensing symposium-IGARSS. IEEE; 2013. p. 3574–7.

[65] Decker M, Brunke MA, Wang Z, Sakaguchi K, Zeng X, Bosilovich MG. Evaluation of the reanalysis products from gsfc, ncep, and ecmwf using flux tower observations. J Clim 2012;25(6):1916–44.

[66] Guo H, Xu M, Hu Q. Changes in near-surface wind speed in China: 1969–2005. Int J Climatol 2011;31(3):349–58.

[67] Gregow H, Jylhä K, Mäkelä H, Aalto J, Manninen T, Karlsson P, Kaiser-Weiss A, Kaspar F, Poli P, Tan D, et al. Worldwide survey of awareness and needs concerning reanalyses and respondents views on climate services. Bull Am Meteorol Soc 2016;97(8):1461–73.

[68] Ramon J, Lledó L, Torralba V, Soret A, Doblas-Reyes FJ. What global reanalysis best represents near-surface winds? Q J R Meteorol Soc 2019;145(724).

[69] Vautard R, Cattiaux J, Yiou P, Thépaut J-N, Ciais P. Northern hemisphere atmospheric stilling partly attributed to an increase in surface roughness. Nat Geosci 2010;3(11):756.

[70] Bichet A, Wild M, Folini D, Schär C. Causes for decadal variations of wind speed over land: sensitivity studies with a global climate model. Geophys Res Lett 2012;39(11).

[71] Wu J, Zha J, Zhao D. Estimating the impact of the changes in land use and cover on the surface wind speed over the east China plain during the period 1980−2011. Clim Dynam 2016;46(3−4):847−63.

[72] Fu G, Yu J, Zhang Y, Hu S, Ouyang R, Liu W. Temporal variation of wind speed in China for 1961−2007. Theor Appl Climatol 2011;104(3−4):313−24.

[73] Troccoli A, Muller K, Coppin P, Davy R, Russell C, Hirsch AL. Long-term wind speed trends over Australia. J Clim 2012;25(1):170−83.

[74] Lin C, Yang K, Qin J, Fu R. Observed coherent trends of surface and upper-air wind speed over China since 1960. J Clim 2013;26(9):2891−903.

[75] Kirchner-Bossi N, García-Herrera R, Prieto L, Trigo RM. A long-term perspective of wind power output variability. Int J Climatol 2015;35(9):2635−46.

[76] England MH, McGregor S, Spence P, Meehl GA, Timmermann A, Cai W, Gupta AS, McPhaden MJ, Purich A, Santoso A. Recent intensification of wind-driven circulation in the pacific and the ongoing warming hiatus. Nat Clim Change 2014;4(3):222.

[77] Helfand HM, Schubert SD. Climatology of the simulated great plains low-level jet and its contribution to the continental moisture budget of the United States. J Clim 1995;8(4):784−806.

[78] Reichler T, Kim J. Uncertainties in the climate mean state of global observations, reanalyses, and the gfdl climate model. J Geophys Res: Atmos. 2008;113(D5).